J. Phys. C: Solid State Phys., **15** (1982) 4547–4557. Printed in Great Britain

Theory of the spin dynamics of paramagnetic EuO and EuS

A P Young† and B S Shastry‡§

† Department of Mathematics, Imperial College, London SW7 2BZ, UK

‡ Department of Physics, University of Utah, Salt Lake City, UT 84112, USA

Received 5 March 1982

Abstract. The method of moments is used to investigate the spin dynamics of paramagnetic EuO and EuS. The theory predicts correctly those wavevectors for which a 'spin wave' peak appears in the spectrum. Furthermore the calculated position of this peak, when one occurs, agrees well with experiment. This suggests that earlier work, in which the same method was applied to an effective Heisenberg model for Fe, was correct in predicting that this model has no 'spin wave' peaks in the wavevector range covered experimentally.

1. Introduction

There has been a great deal of interest in the paramagnetic state of ferromagnetic materials, particularly the transition metals, Ni and Fe. A 'spin wave' peak in the neutron scattering spectrum of Fe (Lynn 1975, 1981) and Ni (Mook *et al* 1973, Lynn and Mook 1981) has been interpreted as evidence for considerable short-range magnetic order (SRMO) above the transition temperature T_c, and many consequences of this assumption of large SRMO have been worked out by Korenman *et al* (1977) and Prange and Korenman (1979). However, it has been argued (Edwards 1980, Shastry *et al* 1981, the latter referred to as SEY), that the observed specific heat and susceptibility of Fe are incompatible with large SRMO. Furthermore, as has been remarked by Als-Nielsen (1976), the correlation length of Fe in the critical region close to T_c is very similar to that of the insulators EuO, EuS whose interactions are known and which do not have vast SRMO above T_c. Also the main features of the 'constant-ω' plots in Lynn (1975) can be explained (SEY) by an effective Heisenberg model for Fe with little SRMO. However, this theory predicts no peaks in 'constant-q' scans in contrast to experiment. It is clearly, therefore, of interest to establish whether this discrepancy is due to the approximations made by SEY in studying Heisenberg model dynamics, or whether some other explanation must be found.

In order to answer this question we have applied precisely the same approximations to EuO and EuS, which are definitely good Heisenberg systems and for which the interactions are accurately known (Bohn *et al* 1980, Mook 1981). Recently neutron scattering experiments (Bohn *et al* 1981, Mook 1981) have been carried out which find a peak in constant-q scans above T_c but only for q close to q_{max}, the zone-boundary

§ Present address: Theoretical Physics Section, Tata Institute of Fundamental Research, Colaba, Bombay, India 400 005.

0022-3719/82/214547 + 11 $01.50

wavevector in the chosen direction, whereas in Fe a peak was observed down to $0.2q_{max}$ (Lynn 1981). Furthermore, the peaks observed in EuO (Mook 1981) are less sharp than those in Fe. (Spectra have not yet been published for EuS, only spin wave energies.) We find that the theory predicts correctly those wavevectors where a 'spin wave' peak occurs in EuO and EuS and also gives an accurate value of the position of this peak. When such a peak is present, the shape of the spectrum is a little inaccurate, in particular the theory tends to underestimate the height of the peak. None the less, the main features of the experimental results are well reproduced by the theory. This gives us confidence that the principal conclusion of SEY is correct; namely that there are no 'spin wave' peaks in the experimental range of q, in an effective Heisenberg model of Fe with reasonable interaction parameters. The discrepancy between theory and Lynn's constant-q plots, therefore, remains.

In § 2 the method of calculation is described and our results are presented in § 3 along with experimental data. Section 4 discusses the significance of the results, while technical details of the computations are relegated to an Appendix.

2. Method

The Heisenberg Hamiltonian for EuO and EuS can be written as

$$H = -\sum_{\langle ij \rangle} J_{ij} \boldsymbol{S}_i \cdot \boldsymbol{S}_j \tag{1}$$

where $\boldsymbol{S}_i$ is an $S = \frac{7}{2}$ operator on site i of an FCC lattice, each distinct pair in equation (1) is counted once and the J_{ij} are exchange interactions. In table 1 we give the experimental values of the nearest neighbour (NN) and next nearest neighbour (NNN) interactions, denoted by J_1 and J_2 respectively. For EuS they were taken from Bohn *et al* (1980) who actually included up to the fifth neighbour couplings in their fit to the low-temperature spin wave data. However, the third to fifth neighbour interactions were found to be very small so we have set them to zero for convenience.

Table 1. J_1 and J_2 are the first- and second-neighbour interactions used in these calculations. For EuO they are taken from Mook (1981) and for EuS they are the values given by Bohn *et al* (1980, 1981). We have neglected the small third to fifth neighbour couplings bound by Bohn *et al*. T_c(expt) is the experimental value of T_c given by Mook and Bohn *et al* while T_c(theory) is our calculated value using the spherical approximation described in the text. T_c^{MF} is the mean field prediction for T_c. All the data are in K.

	J_1	J_2	T_c(expt)	T_c(theory)	T_c^{MF}
EuO	1.25	0.25	69.8	66.5	86.6
EuS	0.442	−0.20	16.6	13.8	21.5

Static properties are evaluated by the spherical approximation in which

$$k_B T \chi(\boldsymbol{q}) = C(\boldsymbol{q}) = \langle S^z(\boldsymbol{q}) S^z(-\boldsymbol{q}) \rangle = \frac{k_B T}{J_0 - J_q + \chi^{-1}}, \tag{2}$$

T is the temperature, k_B is Boltzmann's constant, J_q is the Fourier transform of J_{ij} and $\chi(\boldsymbol{q})$ is the static wavevector-dependent susceptibility. From now on we set k_B, and also $\hbar$, equal to unity, so energies and frequencies will be in units of K. $\chi[\equiv \chi(q = 0)]$ is

determined by the sum rule

$$\frac{1}{N}\sum_{q} C(q) = \tfrac{1}{3}S(S+1). \tag{3}$$

We consider only the paramagnetic phase where correlations are isotropic, i.e. $\langle S^{\alpha}(q)S^{\beta}(-q)\rangle = \delta_{\alpha\beta}C(q)$. In equation (2) the classical fluctuation-dissipation theorem has been used. This is correct if $\omega \ll T$ where ω is a typical fluctuation frequency. It is hence exact at $q = 0$ for any T and spin S, since $S(q = 0)$ is a constant of the motion, and also for $S = \infty$ at any T. It is a very good approximation for all q if $S = \frac{7}{2}$ and $T \geqslant T_c$, the transition temperature, which is the case discussed here. Even for $S = 1$, which is appropriate for Fe, it represents a fairly good approximation above T_c. We note also that the main discrepancy between the theory of SEY and Lynn's (1975, 1981) constant-q plots is a large drop in measured intensity at small ω, where the condition $\omega \ll T$ is well satisfied.

At T_c one has $\chi^{-1} = 0$ so the transition occurs when

$$\frac{1}{N}\sum_{q}\frac{T_c}{J_0 - J_q} = \tfrac{1}{3}S(S+1). \tag{4}$$

Evaluating the q integral numerically by the methods discussed in the Appendix we obtain the values of T_c in table 1. The spherical approximation underestimates T_c somewhat whereas mean field theory, according to which

$$T_c^{MF} = \tfrac{1}{3}S(S+1)J_{q=0}, \tag{5}$$

gives quite a substantial overestimate.

As $q \to 0, J_0 - J_q = 2(J_1 + J_2)(qa_{NN})^2$ where a_{NN} is the nearest-neighbour distance of the FCC lattice. If a is the conventionally defined lattice parameter (e.g. Kittel 1976) then $a_{NN} = a/\sqrt{2}$. Equation (2) therefore has the Ornstein–Zernicke form $C(q) \propto (q^2 + \xi^{-2})^{-1}$ at long wavelengths, where the correlation length, ξ, is given by

$$\xi/a_{NN} = 2(J_1 + J_2)\chi. \tag{6}$$

Results for ξ/a_{NN} at selected temperatures are presented in table 2 for EuO and table 3 for EuS. Consider next the real-space correlation function $\langle S_0^z S_n^z\rangle$ where $n = 1, 2 \ldots$, denotes first, second ... neighbours. With perfect spin alignment this would equal $S(S+1)/3$ so we define a normalised correlation function Γ_n, by

$$\Gamma_n = \frac{3\langle S_0^z S_n^z\rangle}{S(S+1)} = \frac{3}{S(S+1)}\frac{1}{N}\sum_{q}\exp(iq\,.\,R_n)C(q) \tag{7}$$

which has a maximum value of unity. Results for Γ_1 are also shown in tables 2 and 3.

The neutron scattering cross section is proportional to the dynamical structure factor $S(q, \omega)$ where

$$S(q, \omega) = \int_{-\infty}^{\infty} dt\, e^{i\omega t}\langle S^z(q, t)S^z(-q, 0)\rangle. \tag{8}$$

It is much more difficult to obtain reliable time-dependent correlation functions than equal-time averages such as equation (2). Amongst the various approximation schemes the three-pole approximation (e.g. Lovesey and Meserve 1973, Lovesey 1974) seems to us to have been the most successful, so we have used it for these calculations as well as for the earlier work on Fe(SEY). One relates $S(q, \omega)$ to the relaxation shape function

Table 2. (EuO) Γ_1 is the reduced nearest-neighbour correlation function for EuO, normalised to unity for perfect spin alignment, at different values of T/T_c according to the spherical approximation. Interactions used in the calculations are given in table 1. ξ is the magnetic correlation length and a_{NN} is the distance between nearest-neighbour magnetic atoms. q^* is the wavevector beyond which a 'spin wave' peak in the shape function $F(\boldsymbol{q}, \omega)$ is observed as a function of ω for fixed $\boldsymbol{q}$. The results shown are for $\boldsymbol{q}$ in the (1, 1, 1) direction and are presented as a fraction of q_{max}, the zone-boundary wavevector in this direction. The experimental results are from Mook (1981). ω_{SW} is the energy of the 'spin wave' peak in K and results are presented for $q = q_{max}$ in the (1, 1, 1) direction. The agreement between theory and experiment is most satisfactory. The experimental values of ω_{SW} are the maxima of Mook's fits to his data, the full curves in figure 2 of Mook (1981).

T/T_c	Γ_1	ξ/a_{NN}	q^*/q_{max} (1, 1, 1)		ω_{SW} (1, 1, 1) $q = q_{max}$	
			Theory	Expt	Theory	Expt
1.0	0.239	∞	0.68	Between 0.5 and 1.0	32.5	32
1.27	0.136	1.32	0.76	Between 0.5 and 1.0	25.0	25
2.0	0.066	0.55	0.82	Between 0.5 and 1.0	20.0	23

Table 3. (EuS) Same as for table 2 except that data refer to EuS, the wavevectors are in the (1, 0, 0) direction, and the experimental results are from Bohn *et al* (1981).

T/T_c	Γ_1	ξ/a_{NN}	q^*/q_{max} (1, 0, 0)		ω_{SW} (1, 0, 0)			
					$q = q_{max}$		$q = 0.8q_{max}$	
			Theory	Expt	Theory	Expt	Theory	Expt
1.0	0.317	∞	0.63	Between 0.6 and 0.8	15.5	15	13.5	11.5
1.5	0.157	0.86	0.68	Between 0.6 and 0.8	11.5	12	10.0	8.5

$F(\boldsymbol{q}, \omega)$ in the standard way

$$S(\boldsymbol{q}, \omega) = \frac{\omega}{1 - e^{-\beta\omega}} \chi(\boldsymbol{q}) F(\boldsymbol{q}, \omega) \tag{9}$$

and $F(\boldsymbol{q}, \omega)$ is then approximated by

$$F(\boldsymbol{q}, \omega) = \frac{1}{\pi} \frac{\tau\delta_1\delta_2}{[\omega\tau(\omega^2 - \delta_1 - \delta_2)]^2 + (\omega^2 - \delta_1^2)^2} \tag{10}$$

where

$$\delta_1 = \langle\omega^2\rangle_q \qquad \delta_1\delta_2 = \langle(\omega^2 - \langle\omega^2\rangle_q)^2\rangle_q \tag{11}$$

$$\tau = (\pi\delta_2/2)^{-1/2}.$$

$\langle\omega^2\rangle_q$ and $\langle\omega^4\rangle_q$ are the second and fourth frequency moments of F which can be expressed in terms of static correlation functions (Marshall and Lovesey 1971). In particular

$$\langle\omega^2\rangle_q = \frac{2}{\chi(q)} \frac{1}{N} \sum_p C(\boldsymbol{p})(J_p - J_{q-p}). \tag{12}$$

$\langle\omega^4\rangle_q$ is given in terms of four-spin correlation functions, which, following Lovesey and Meserve (1973), we approximate by products of two-spin correlation functions given by equation (2). We find that

$$\langle\omega^4\rangle_q = \frac{2}{\chi(q)}\frac{1}{N^2}\sum_{k,p} C(k)C(p)(J_{q-k}-J_k)\{(J_p - J_{q-k-p})[(J_{q-p}-J_p)+2(J_{q-k}-J_k)] + 2(J_k - J_q)(J_{q-p}-J_p) + (J_p - J_k)(J_{k+p}-J_{q-k-p})\}. \tag{13}$$

The method of evaluating the double wavevector sums in equation (13) is summarised in the Appendix. The shape function $F(q, \omega)$ in equation (10) has either one peak, at $\omega = 0$, if $\delta_2 > 2\delta_1$ or three peaks, at $\omega = 0$ and $\omega = \pm\omega_{SW}$, if $\delta_2 < 2\delta_1$. We shall call the maximum at $\omega = \omega_{SW}$ (ω_{SW} is a rather complicated function of the δs) the 'spin wave' peak. In the next section it will be seen that such a peak can appear even when there is little SRMO (they are of course then rather broad and not very high) so the terminology 'spin wave' may be somewhat inappropriate.

3. Results and comparison with experiment

First of all we describe the available experimental data. For EuO Mook (1981) presents spectra for the relaxation function $R(q, \omega) = \chi(q)F(q, \omega)$ at $T/T_c = 1.0$, 1.27 and 2.0. At each of these temperatures 'spin wave' peaks are seen in the (1, 1, 1) direction for $q/q_{max} = 1.0$ but not for $q/q_{max} = 0.5$ where q_{max} is the zone-boundary wavevector in the direction considered. In the case of EuS, Bohn *et al* (1981) do not present spectra but give the frequencies of 'spin waves' where they exist. From their figure 2 one infers that 'spin waves' occur in the (1, 0, 0) direction at $T/T_c = 1.0$ and 1.5 for $q/q_{max} = 0.8$ and 1.0 but not for $q/q_{max} \leqslant 0.6$. This information is summarised in tables 2 and 3.

Denoting by q^* the wavevector beyond which peaks appear we have calculated q^* for EuO and EuS for the relevant temperatures and directions. We have also calculated the 'spin wave' energy ω_{SW}, when a 'spin wave' peak appears, and present this information in tables 2 and 3 alongside the corresponding experimental results. Clearly the theory is rather successful in predicting where peaks appear and also gives quite accurately the 'spin wave' energies. This success suggests that the method may in general be accurate in predicting the existence or otherwise of paramagnetic 'spin waves' and gives additional confidence in the main results of SEY.

Notice the nearest-neighbour correlation function Γ_1, for EuO, is very small at $T/T_c = 2.0$, where a rather broad peak is found experimentally and theoretically. This shows that strong SRMO is not necessary to get a peak in the response. A more extreme case is for EuS with $q = q_{max}$ in the (1, 0, 0) direction where the calculated peak persists up to $T = \infty$, at which there are no correlations at all. We therefore feel that the word 'spin wave' is rather misleading when used to describe such broad features. In certain cases the equations of motion themselves can give such a peak, which may then be enhanced by SRMO.

We believe that persistence of peaks in the (1, 0, 0) direction of EuS is due to the second-neighbour interaction, J_2, being negative. It appears that 'compensation' of this sort can increase the likelihood of 'spin waves' and it should be noted that the second-neighbour bonds are along the (1, 0, 0) direction. This suggests that different behaviour may occur in the (1, 1, 1) direction and indeed our calculations find no spin waves at all in this case. It would be interesting to check this prediction by experiment. Values of

Table 4. (EuS). Calculated values of δ_1 and δ_2 (in units of K^2, where $k_B = \hbar = 1$) for EuS at different temperatures, directions and for different values of q/q_{max}, where q_{max} is the zone-boundary wavevector in the chosen direction. The calculated shape function can easily be obtained from equation (10) of the text once δ_1 and δ_2 are known. A 'spin wave' peak appears if $\delta_2 < 2\delta_1$.

		(1, 0, 0)		(1, 1, 1)		(1, 1, 0)	
q/q_{max}	T/T_c =	1.25	1.75	1.25	1.75	1.25	1.75
0.25	δ_1	1.69	2.39	0.928	1.57	1.85	2.64
	δ_2	54.0	56.2	50.3	54.2	53.9	56.5
0.50	δ_1	21.2	17.9	8.24	8.85	18.1	16.5
	δ_2	83.6	73.2	67.2	65.9	79.7	73.0
0.75	δ_1	75.8	54.0	22.7	21.0	54.7	42.6
	δ_2	121.0	91.3	85.3	77.9	109.0	88.3
1.0	δ_1	113.0	77.1	30.8	27.5	92.5	66.1
	δ_2	140.0	99.0	93.3	83.0	130	96.4

δ_1 and δ_2 for different directions are given in table 4. For EuO, where J_2 is positive, there is a much smaller difference between our results in the two directions, see table 5. From equation (10) and the data in tables 4 and 5 it is trivial to construct the shape function for different directions and temperatures. We hope this will stimulate experimentalists to perform new measurements in other directions to test our predictions.

A more severe test of the theory, which is, however, not necessary for the main conclusions of SEY, is to compare the shape of the spectrum with the experimental data. In figure 1 we show the calculated shape function $F(\boldsymbol{q}, \omega)$ and experimental points (Mook 1981) for EuO at $T = 1.27T_c$ with $\boldsymbol{q}$ in the (1, 1, 1) direction for $q = 0.5q_{max}$ and $q = q_{max}$. The vertical scale is arbitrary. For $q = 0.5q_{max}$, where no 'spin waves' are found, the theory agrees fairly well with experiment. However, for $q = q_{max}$, where a 'spin wave' peak is seen the theoretical curve rises at low ω whereas the experimental points decrease. This has the effect of making the experimental peak more pronounced than in the theory. None the less, we emphasise that the theory predicts well the wavevectors at which peaks appear and gives the shape of the spectrum reasonably well when 'spin waves' are not predicted. Furthermore, when 'spin waves' appear, the peak positions, although not their height, are accurately given by the theory.

Table 5. (EuO). As table 4, but for EuO.

		(1, 0, 0)		(1, 1, 1)		(1, 1, 0)	
q/q_{max}	T/T_c =	1.25	1.75	1.25	1.75	1.25	1.75
0.25	δ_1	23.3	27.2	14.9	19.1	28.1	31.4
	δ_2	378.0	370.0	353.0	353.0	386.0	374.0
0.50	δ_1	194.0	157.0	128.0	108.0	228.0	178.0
	δ_2	612.0	513.0	523.0	455.0	630.0	518.0
0.75	δ_1	486.0	355.0	352.0	259.0	528.0	377.0
	δ_2	863.0	658.0	711.0	560.0	870.0	652.0
1.0	δ_1	632.0	452.0	476.0	339.0	652.0	461.0
	δ_2	971.0	718.0	794.0	604.0	973.0	712.0

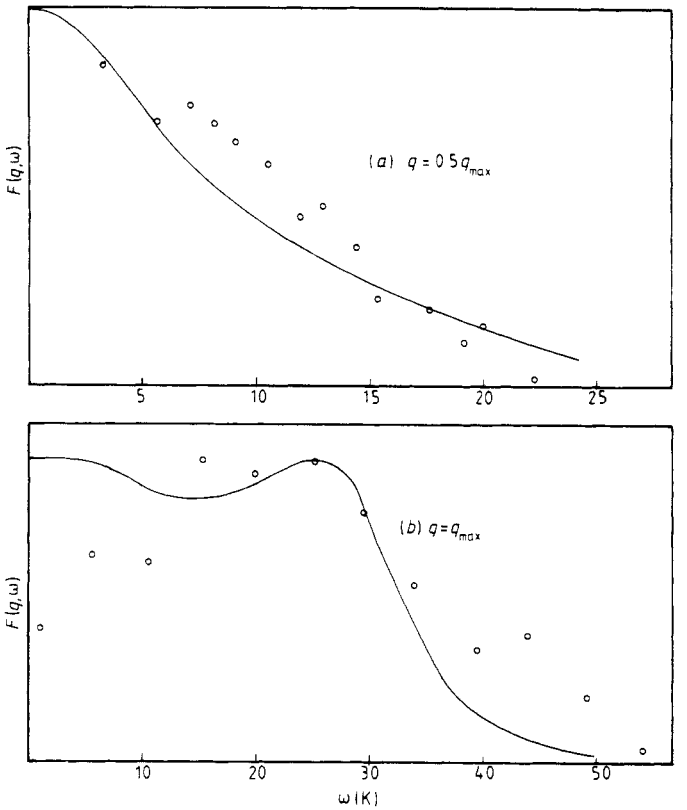

Figure 1. Full curves are the calculated relaxation shape function $F(\boldsymbol{q}, \omega)$ for EuO at $T = 1.27T_c$ with $\boldsymbol{q}$ in (1, 1, 1) direction. Upper curve is for $q = 0.5q_{max}$ and the lower is for $q = q_{max}$, where q_{max} is the zone-boundary wavevector in this direction. The vertical scale is arbitrary. The circles are the experimental results of Mook (1981) for $F(\boldsymbol{q}, \omega)$, again in arbitrary units. The calculated curves are from equation (10) of the text, with, in units of K^2, curve (*a*) $\delta_1 = 127$, $\delta_2 = 518$; curve (*b*) $\delta_1 = 465$, $\delta_2 = 779$.

4. Discussion

The main conclusion is that the three-pole approximation is rather successful in predicting when peaks appear in the spectrum of a ferromagnetically coupled Heisenberg system above T_c. To be precise we refer to peaks in the shape function $F(\boldsymbol{q}, \omega)$ as a function of ω at fixed $\boldsymbol{q}$. The method also gives quite accurately the energy of these peaks, when they occur. It is less successful in predicting the detailed shape of the spectrum in the spin wave region.

The agreement between experiment and our calculations on EuS and EuO, gives us confidence in the results of SEY who applied the same approximations to an effective Heisenberg model of Fe. Their main conclusion is that such a model, with reasonable interaction parameters, has little SRMO and no 'spin wave' peaks above T_c in the experimental range of $\boldsymbol{q}$. One is therefore led to the conclusion that the peaks observed by Lynn (1975, 1981) must be due to some, as yet not understood, itinerant effect. This is puzzling because Edwards (1982) has argued that itinerant contributions should be small for Fe, which is predicted to have good local moments (Hasegawa 1979, Hubbard 1979a,

b). At the same time the hypothesis of large SRMO (Korenman *et al* 1977, Prange and Korenman 1979) seems incompatible with the susceptibility (SEY) and also with correlation length in the critical region. Furthermore, recent calculations on itinerant models (Hasegawa 1981, Moriya 1982) find only a small amount of SRMO above T_c, consistent with the Heisenberg calculations of SEY. In fact, Wang *et al* (1982) (see also Prange 1981) and You *et al* (1980) have calculated the exchange parameters of an effective Heisenberg model of Fe starting from a microscopic (i.e. itinerant) picture. Wang *et al* find that the resulting model has little SRMO above T_c. The interactions given by You *et al* actually lead to a negative spin wave stiffness, D, at $T = 0$, although including s bands in the calculation rectifies this defect. SEY argue that any set of interactions which does not have an anomalously small D should have little SRMO above T_c. Consequently there is no theory at present which predicts, rather than assumes, large SRMO.

It seems that more experimental and theoretical work is needed to clarify this confusing situation for Fe. For EuO and EuS, however, we believe that our calculation provides a quantitative theory for the existing experiments. It may also provide an impetus for further experiments designed to scan other directions in $\boldsymbol{q}$-space, in order to verify our predictions.

Acknowledgments

We would like to thank Dr D M Edwards for many helpful discussions.

Appendix

In this Appendix we discuss how the wavevector sums are evaluated numerically. We use a cubic Brillouin zone which actually contains twice each wavevector of the FCC zone but has the advantage that the range of integration is simple. If a is the standard lattice parameter of the FCC lattice (e.g. Kittel 1976) then each wavevector component is integrated from $-2\pi/a$ to $2\pi/a$. The NN spacing a_{NN} is related to a by $a_{NN} = a/\sqrt{2}$.

J_q is given by

$$J_q = 4J_1[\cos(q_x a/2)\cos(q_y a/2) + \cos(q_y a/2)\cos(q_z a/2) + \cos(q_z a/2)\cos(q_x a/2)] + 2J_2[\cos(q_x a) + \cos(q_y a) + \cos(q_z a)] \qquad \text{(A1)}$$

so evaluation of the static two-spin correlation functions in equation (2) requires integrals of the type

$$\frac{1}{N}\sum_{q}^{\text{FCC zone}} f(\cos(q_x a/2), \cos(q_y a/2), \cos(q_z a/2))$$

which can be manipulated to give

$$\int_{-\pi}^{\pi} \frac{dx}{2\pi}\frac{dy}{2\pi}\frac{dz}{2\pi} f(\cos x, \cos y, \cos z). \qquad \text{(A2)}$$

Each integral in (A2) is performed by Gauss–Chebyshev quadrature, i.e. for each component

$$\int_{-\pi}^{\pi} \frac{dx}{2\pi} g(\cos x) \simeq \frac{1}{m} \sum_{i=1}^{m} g(\cos x_i) \tag{A3}$$

where

$$x_i = (2i - 1)\pi/2m. \tag{A4}$$

Later we shall need to integrate functions of sines as well as cosines for which the equation analagous to equation (A3) is

$$\int_{-\pi}^{\pi} \frac{dx}{2\pi} g(\cos x, \sin x) \simeq \frac{1}{2m} \sum_{i=1}^{2m} g(\cos x_i, \sin x_i) \tag{A5}$$

where x_i is still given by equation (A4).

Thus m^3 points have to be evaluated for the three-dimensional integral (A2) and $(2m)^3$ points are needed if the integral involves sines. The method is very accurate, even for fairly small values of m, except at T_c where the vanishing of the denominator in equation (2) for $q = 0$ makes convergence slow. In this case one can show that the leading error varies as m^{-1}. Hence by evaluating the integral for $m = n$ and $2n$ and forming the combination $2I_{2n} - I_n$ the leading error is eliminated and convergence is much more rapid.

The second moment, given by equation (12), is easily evaluated. Writing

$$\langle \omega^2 \rangle_q = [2/\chi(\boldsymbol{q})]\rho_q \tag{A6}$$

then

$$\rho_q = \frac{1}{N} \sum_{p} C(\boldsymbol{p})(J_p - J_{q-p}) = \sum_{j} J_{ij}[1 - \cos(\boldsymbol{q} \cdot \boldsymbol{R}_{ij})]\langle S_j^z S_i^z \rangle. \tag{A7}$$

Since only NN and NNN interactions are included ρ_q is obtained simply for all $\boldsymbol{q}$ once Γ_1 and Γ_2 have been evaluated.

The fourth moment is more complicated. To save computer time we shall manipulate equation (13) so that only single wavevector summations are necessary. Equation (13) breaks up naturally into a sum of four terms so we write

$$\langle \omega^4 \rangle_q = (2/\chi_q)(A_1 + A_2 + A_3 + A_4). \tag{A8}$$

Consider A_3 first of all:

$$\begin{aligned} A_3 &= \frac{2}{N^2} \sum_{k,p} C(\boldsymbol{k})C(\boldsymbol{p})(J_{q-k} - J_k)(J_k - J_q)(J_{q-p} - J_p) \\ &= \frac{-2}{N} \rho_q \sum_{k} C(\boldsymbol{k})(J_{q-k} - J_k)(J_k - J_q) \\ &= -2\rho_q^2 J_q - 2\rho_q \frac{1}{N} \sum_{k} C(\boldsymbol{k})(J_{q-k} - J_k)J_k. \end{aligned} \tag{A9}$$

Now

$$\begin{aligned} &\frac{1}{N} \sum_{k} C(\boldsymbol{k})(J_{q-k} - J_k)J_k \\ &= \frac{1}{N} \sum_{k} C(\boldsymbol{k})(J_{q-k} - J_k)(J_k - J_0 - \chi^{-1} + \chi^{-1} + J_0) \\ &= -(\chi^{-1} + J_0)\rho_q \end{aligned} \tag{A10}$$

using equation (2) and the fact that the average over $\boldsymbol{k}$ of $J_k - J_{q-k}$ is zero. From (A9) and (A10) one has

$$A_3 = 2\rho_q^2(\chi^{-1} + J_0 - J_q) \tag{A11}$$

which does not involve any further integrals once ρ_q and χ^{-1} are known.

Next we discuss A_4, which is given by

$$A_4 = \frac{1}{N^2}\sum_{k,p} C(\boldsymbol{k})C(\boldsymbol{p})(J_{q-k} - J_k)(J_p - J_k)(J_{k+p} - J_{q-k-p}). \tag{A12}$$

From equation (2) we have

$$C(\boldsymbol{k})C(\boldsymbol{p})(J_p - J_k) = T[C(\boldsymbol{p}) - C(\boldsymbol{k})]. \tag{A13}$$

The term in (A13) involving $C(\boldsymbol{k})$ gives zero when substituted into (A12). Fourier transforming the remaining term then gives

$$A_4 = -2T\sum_j J_{ij}^2[1 - \cos(\boldsymbol{q}\,.\,\boldsymbol{R}_{ij})]\langle S_i^z S_j^z\rangle \tag{A14}$$

which again does not involve any new integrals.

A_2 is given by:

$$\begin{aligned} A_2 &= \frac{2}{N^2}\sum_{k,p} C(\boldsymbol{k})C(\boldsymbol{p})(J_{q-k} - J_k)^2(J_p - J_{q-k-p}) \\ &= \frac{2}{N}\sum_k C(\boldsymbol{k})(J_{q-k} - J_k)^2\rho_{q-k} \end{aligned} \tag{A15}$$

which only involves a single three-dimensional sum over $\boldsymbol{k}$. J_{q-k} and ρ_{q-k} can be expressed in terms of $\cos(k_x^i a/2)$ and $\sin(k^i a/2)$, $i = x, y$ or z, so each of the three components of $\boldsymbol{k}$ can be integrated as in equation (A5).

A_1 is the most complicated term. It is given by

$$A_1 = \frac{1}{N^2}\sum_{k,p} C(\boldsymbol{k})C(\boldsymbol{p})(J_{q-k} - J_k)(J_p - J_{q-k-p})(J_{q-p} - J_p). \tag{A16}$$

From equation (A10) this can be rearranged to yield

$$A_1 = (\chi^{-1} + J_0)\rho_q^2 + A_1' \tag{A17}$$

where

$$A_1' = \frac{1}{N^2}\sum_{k,p} \mathscr{C}_q(\boldsymbol{k})\mathscr{C}_p(\boldsymbol{k})J(\boldsymbol{k} + \boldsymbol{p}) \tag{A18}$$

with

$$\mathscr{C}_q(k) = (J_{k+q/2} - J_{k-q/2})C(\boldsymbol{k} + \boldsymbol{q}/2). \tag{A19}$$

$J(\boldsymbol{k} + \boldsymbol{p})$ is a function of the $\cos[(k^i + p^i)a/2]$, $i = x, y$ or z. The cosines are expanded so A_1' is written as a sum of terms, each of which is a product of two *independent* sums over k, i.e.

$$\begin{aligned} A_1' = 4J_1[&-\langle\!\langle\cos(k_x a/2)\cos(k_y a/2)\rangle\!\rangle^2 - \langle\!\langle\sin(k_x a/2)\sin(k_y a/2)\rangle\!\rangle^2 \\ &+ \langle\!\langle\cos(k_x a/2)\sin(k_y a/2)\rangle\!\rangle^2 + \langle\!\langle\sin(k_x a/2)\cos(k_y a/2)\rangle\!\rangle^2 \\ &+ 8 \text{ terms from permuting cartesian indices}] \end{aligned}$$

$$+ 2J_2[-\langle\langle\cos(k_x a)\rangle\rangle^2 + \langle\langle\sin(k_x a)\rangle\rangle^2$$

$$+ 4 \text{ terms from permuting cartesian indices}] \tag{A20}$$

where

$$\langle\langle f(\boldsymbol{k})\rangle\rangle = \frac{1}{N}\sum_{\boldsymbol{k}} f(\boldsymbol{k})\mathcal{C}_q(\boldsymbol{k}). \tag{A21}$$

$\mathcal{C}_q(k)$ can be expressed in terms of the $\cos(k^i a/2)$, $\sin(k^i a/2)$. Hence each of the averages in (A20) is a three-dimensional integral, each component of which is evaluated according to equation (A5).

The final expression for the fourth moment is obtained by combining equations (A8), (A11), (A12), (A13), (A14) and (A20).

Note added in proof. After this paper was submitted for publication we were informed of work by Lindgård (1982), who has also investigated Heisenberg model dynamics by a moments approach. He used a 'two-pole' approximation, in which the shape function is cut off at a frequency determined by the fourth moment. There are a number of other technical differences between his approach and ours but both methods give a reasonably good description of the dynamics of EuO. Lindgard also notes that the opposite sign of J_2 for EuS leads to significantly different results.

References

Als-Nielsen J 1976 *Phase Transitions and Critical Phenomena* vol. 5A ed. C Domb and M S Green (New York: Academic Press) pp 139–45

Bohn H G, Zinn W, Dorner B and Kollmar A 1980 *Phys. Rev.* B **22** 5447

—— 1981 *J. Appl. Phys.* **52** 2228

Edwards D M 1980 *J. Magn. Magn. Mater.* **15–18** 262

—— 1982 *J. Phys. F: Met. Phys.* **12** 1789

Hasegawa H 1979 *J. Phys. Soc. Japan* **46** 1504

—— 1981 *Solid State Commun.* **38** 401

Hubbard J 1979a *Phys. Rev.* B **19** 2626

—— 1979b *Phys. Rev.* B **20** 4584

Kittel C 1976 *Introduction to Solid State Physics* 5th edn (New York: Wiley)

Korenman V, Murray J L and Prange R E 1977 *Phys. Rev.* B **16** 4032, 4048, 4058

Lindgård P A 1982 *J. Appl. Phys.* **53** 1861

Lovesey S W 1974 *J. Phys. C: Solid State Phys.* **7** 2008

Lovesey S W and Meserve R A 1973 *J. Phys. C: Solid State Phys.* **6** 79

Lynn J W 1975 *Phys. Rev.* B **11** 2624

—— 1981 *Physics of Transition Metals 1981* (Inst. Phys. Conf. Ser. 55) p 683

Lynn J W and Mook H A 1981 *Phys. Rev.* B **23** 198

Marshall W and Lovesey S W 1971 *Theory of Thermal Neutron Scattering* (Oxford: Oxford University Press)

Mook H A 1981 *Phys. Rev. Lett.* **46** 508

Mook H A, Lynn J W and Nicklow R M 1973 *Phys. Rev. Lett.* **30** 556

Moriya T 1982 *J. Phys. Soc. Japan* **51** 420

Prange R E 1981 *Electron Correlation and Magnetism in Narrow-Band Systems* ed. T Moriya (*Springer Series in Solid-State Science 29*) p 63

Prange R E and Korenman V 1979 *Phys. Rev.* B **19** 4691, 4698

Shastry B S, Edwards D M and Young A P 1981 *J. Phys. C: Solid State Phys.* **14** L665

Wang C S, Prange R E and Korenman V 1982 preprint

You M V, Heine V, Holden A J and Lin-Chung P J 1980 *Phys. Rev. Lett.* **44** 1282